



Calhoun: The NPS Institutional Archive

Theses and Dissertations

Thesis Collection

1984

Fin-line Horn Antennas.

Musitano, John Raymond

Monterey, California. Naval Postgraduate School

<http://hdl.handle.net/10945/19345>



Calhoun is a project of the Dudley Knox Library at NPS, furthering the precepts and goals of open government and government transparency. All information contained herein has been approved for release by the NPS Public Affairs Officer.

Dudley Knox Library / Naval Postgraduate School
411 Dyer Road / 1 University Circle
Monterey, California USA 93943

<http://www.nps.edu/library>

NAVAL POSTGRADUATE SCHOOL

Monterey, California



THESIS

FIN-LINE
HORN ANTENNAS

by

John Raymond Musitano

December 1984

Thesis Advisor:

J. B. Knorr

Approved for public release; distribution unlimited

T223001

REPORT DOCUMENTATION PAGE		READ INSTRUCTIONS BEFORE COMPLETING FORM
1. REPORT NUMBER	2. GOVT ACCESSION NO.	3. RECIPIENT'S CATALOG NUMBER
4. TITLE (and Subtitle) Fin-Line Horn Antennas		5. TYPE OF REPORT & PERIOD COVERED Master's Thesis; December 1984
		6. PERFORMING ORG. REPORT NUMBER
7. AUTHOR(s) John Raymond Musitano		8. CONTRACT OR GRANT NUMBER(s)
9. PERFORMING ORGANIZATION NAME AND ADDRESS Naval Postgraduate School Monterey, California 93943		10. PROGRAM ELEMENT, PROJECT, TASK AREA & WORK UNIT NUMBERS
11. CONTROLLING OFFICE NAME AND ADDRESS Naval Postgraduate School Monterey, California 93943		12. REPORT DATE December 1984
		13. NUMBER OF PAGES 46
14. MONITORING AGENCY NAME & ADDRESS (if different from Controlling Office)		15. SECURITY CLASS. (of this report) UNCLASSIFIED
		15a. DECLASSIFICATION/DOWNGRADING SCHEDULE
16. DISTRIBUTION STATEMENT (of this Report) Approved for public release; distribution unlimited		
17. DISTRIBUTION STATEMENT (of the abstract entered in Block 20, if different from Report)		
18. SUPPLEMENTARY NOTES		
19. KEY WORDS (Continue on reverse side if necessary and identify by block number) Fin-Line Horn Antenna; Printed Circuit Antenna		
20. ABSTRACT (Continue on reverse side if necessary and identify by block number) A new, bilateral fin-line horn antenna is introduced and the results of testing discussed. Experimental return loss and absolute gain data are presented and used to make comparisons between the characteristics of conventional and fin-line horns. Classical analysis assuming Huygen source distribution and E-Plane sectoral horn modeling is applied with limited success.		

Approved for public release; distribution is unlimited.

**Fin-line
Horn Antennas**

by

John R. Musitano
Lieutenant Commander, United States Navy Reserve
B.S., United States Naval Academy, 1965

Submitted in partial fulfillment of the
requirements for the degree of

MASTER OF SCIENCE IN ELECTRICAL ENGINEERING

from the

NAVAL POSTGRADUATE SCHOOL
December 1984

ABSTRACT

A new, bilateral fin-line horn antenna is introduced and the results of testing discussed. Experimental return loss and absolute gain data are presented and used to make comparisons between the characteristics of conventional and fin-line horns. Classical analysis assuming Huygen source distribution and E-plane sectoral horn modeling is applied with limited success.

TABLE OF CONTENTS

I.	INTRODUCTION	8
	A. BACKGROUND	8
	B. RELATED WORK	8
	C. PURPOSE	9
II.	THEORY	10
	A. GENERAL	10
III.	EXPERIMENTAL APPROACH	11
	A. TEST STRUCTURE	11
	B. DATA SETS	12
IV.	EXPERIMENTAL APPARATUS AND MEASUREMENT	
	PROCEDURES	14
	A. TEST SYSTEM	14
	B. PROCEDURES	18
	1. Return Loss	18
	2. Absolute Gain	18
	3. Radiation Patterns	19
V.	ANALYSIS	22
	1. Return Loss Analysis	32
	2. Gain Analysis	32
	3. Radiation Pattern Analysis	37
VI.	CONCLUSIONS AND RECOMMENDATIONS	43
	LIST OF REFERENCES	45
	INITIAL DISTRIBUTION LIST	46

LIST OF TABLES

1. Antenna Dimensions For Each Flare Angle 37
2. Small B Antenna Pattern Characteristics 38

LIST OF FIGURES

3.1	Sketch of Test Antennas	13
4.1	Test Set-up	15
4.2	Photo of Test Antennas	16
4.3	Photo of Test Fixture	16
4.4	Photo of Test Fixture with With Test Antenna . . .	17
4.5	Photo of Test Fixture with Ground Plane	17
4.6	Typical Return Loss Plot: 40° Flare Angle and Small B Antenna	20
4.7	Typical Absolute Gain Plot: 40° Flare Angle and Small B Antenna	21
5.1	Gain Analysis Plot for Small A Antenna	23
5.2	Gain Analysis Plot for Large A Antenna	24
5.3	Gain Analysis Plot for Small B Antenna	25
5.4	Gain Analysis Plot for Large B Antenna	26
5.5	Gain Analysis Plot for Small A Antenna Plus Ground Plane	27
5.6	Gain Analysis Plot for Large A Antenna Plus Ground Plane	28
5.7	Gain Analysis Plot for Small B Antenna Plus Ground Plane	29
5.8	Gain Analysis Plot for Large B Antenna Plus Ground Plane	30
5.9	Gain Analysis Plot for 40 Degree Flare Angle . . .	31
5.10	Sketch Showing Fin-line Horn Dimensions	34
5.11	E-Plane Radiation Pattern for Small B at 40° Flare Angle	39
5.12	H-Plane Radiation Pattern for Small B at 40° Flare Angle	40

5.13	E-Plane Radiation Pattern for Small B + G.P. at 40° Flare Angle	41
5.14	H-Plane Radiation Pattern for Small B + G.P. at 40° Flare Angle	42

I. INTRODUCTION

A. BACKGROUND

Millimeter wave integrated circuits have grown in prominence in recent years with the largest impetus coming from the promise of superior performance in defense systems. Potential applications have spurred development of various components that have the advantage of simplicity of design, ease of manufacture, low insertion loss and compatibility with hybrid IC devices. Integrated fin-line has been identified as a promising transmission line and various circuits using this structure have been reported [Ref. 1]. These include a wide-band high-isolation low-loss SPST switch, a balanced mixer, a four-port coupler and an endfire antenna [Ref. 2]. This paper will introduce a new, bilateral fin-line horn antenna and give the experimental results of testing.

B. RELATED WORK

Meier introduced a unilateral, integrated fin-line antenna that operated at 35 GHz [Ref. 2]. This endfire device was constructed in fin-line by extending the printed card beyond the WR-28 waveguide housing. He reported that the shape of the endfire radiation pattern could be varied by changing the geometry of the printed circuit or by varying the aperture of the housing. Since his investigation was limited in scope only minimal data was taken and no theoretical analysis offered. The test results showed measured gain to be 13.5 dBi, well above that of empty, open ended waveguide, and offered promise for possible use of fin-line as antennas.

Encouraged by Meier's results, J.B. Knorr designed three bi-lateral fin-line horn antennas and examined their characteristics. The antennas were manufactured using photoetching techniques from .125 inch, double clad Rexolite 1422 and had fixed flare angles of 30°, 45° and 60°. Investigation consisted of antenna pattern measurements that were conducted in a hairflex-lined anechoic chamber using a klystron power source operating at approximately 8.2 GHz. E and H-plane patterns were taken and gain measured with the aid of a Microline 56X1 standard gain horn and a precision variable attenuator. Knorr demonstrated that the antennas could provide up to 11.1 dBi of gain with a 30° flare angle. For this angle the E and H-plane half-power beam widths were measured as 20° and 32° respectively.

C. PURPOSE

Although several theoretical treatises have discussed the theory of operation of fin-line components, very little experimental work has been reported that examined fin-line antennas. In general the goals of collecting and analyzing experimental results are to construct and/or verify theoretical modeling of heretofore untested designs. The hope is to verify existing theory or propose modifications to more closely explain the observed results and thus improve the accuracy of predicted behavior.

The purpose of this paper is to present the results of a carefully planned series of experiments employing a structured approach to examine the behavior of fin-line horn antennas. The experimental approach, test facilities and analysis will be discussed in detail and some results of modeling revealed.

II. THEORY

A. GENERAL

Since very little experimental work has been done in the area of fin-line antennas there is a corresponding paucity of theoretical discussions in the literature. In general, fin-line horns are thought to behave like aperture antennas but questions arise as to what model might be applied to predict their characteristics. For this treatise, the behavior of the fin-line horn was considered analogous to that of a three dimensional sectoral or pyramidal horn. The test antennas were mounted vertically in WR(90) slotted waveguide to allow the E-field to induce fields across the enclosed fin-line feed of the horns. Like the three dimensional horn, the flared end of the fin-line antenna provides a transition to free space.

In general, integrated fin-line components are considered most useful at millimeter wave frequencies. However, because of mounting limitations and available test facilities, testing was performed for frequencies from 8 to 12 GHz inclusive. Scaling will permit predicted behavior for higher frequency bands.

III. EXPERIMENTAL APPROACH

A. TEST STRUCTURE

Meier and Knorr both showed that fin-line antennas could provide gain well in excess of that provided by an open empty waveguide. Their work also prompted questions regarding optimal design. Specifically, and with regard to on-axis gain:

- Is there an optimal flare angle?
- How does gain vary with antenna metal surface area and flare angle?
- How does gain vary with end termination i.e. how does gain differ between antennas where the metal terminates abruptly versus those that end with dielectric?
- What effects will a ground plane have on the characteristics of the antennas?

Also, with respect to radiation patterns:

- How does half-power beam width, sidelobe position and sidelobe level vary with flare angle, surface area and end termination?

To investigate these questions in a structured manner while using the minimum number of test articles, it was decided to manufacture four antennas from .125 mil, copper plated, double clad, .125 inch Rexolite 1422 having a dielectric constant of 2.3 - 2.5. Two basic designs were chosen with approximately 200 cm² and 300 cm² surface area each. After etching, the dielectric was trimmed to create two different end terminations. For two of the antennas, one with 200 cm² and the other with 300 cm² surface area, the dielectric was trimmed so that the antennas ended abruptly with metal. These antennas were designated "Small

A" and "Large A" respectively. For the remaining two antennas, one small and the other large, the dielectric was trimmed so as to retain about 1.3 cm on the ends. These two antennas were designated "Small B" and "Large B". All four antennas were etched with a 0° flare angle. See Figure 3.1.

B. DATA SETS

Experimental investigation of the antennas began with data recorded at 0° flare angle for each antenna. Upon completion of the data set for this flare angle, all four antennas were modified to a 10° flare angle bi-laterally. This was accomplished by measuring with a protractor and trimming with a sharp knife. A data set was then taken for the 10° flare angle. Like procedures produced data sets for 20° , 30° , 40° , 50° and 60° . To provide a baseline for comparison, data sets were also taken for open waveguide and waveguide with unextended fin-line having $w/b = .236/1.016$ or $w/b = .23223$.

Complete data sets included return loss, absolute gain and E/H-Plane radiation patterns. Return loss and on-axis absolute gain data was taken using a computer controlled scalar network analyzer with a swept frequency source that covered the frequencies from 8 to 12 GHz. The on-axis absolute gain values were examined to determine the frequency of maximum gain and then the E and H-Plane radiation patterns taken at that frequency. All radiation patterns were recorded along with that of the standard gain horn for ease of comparison.

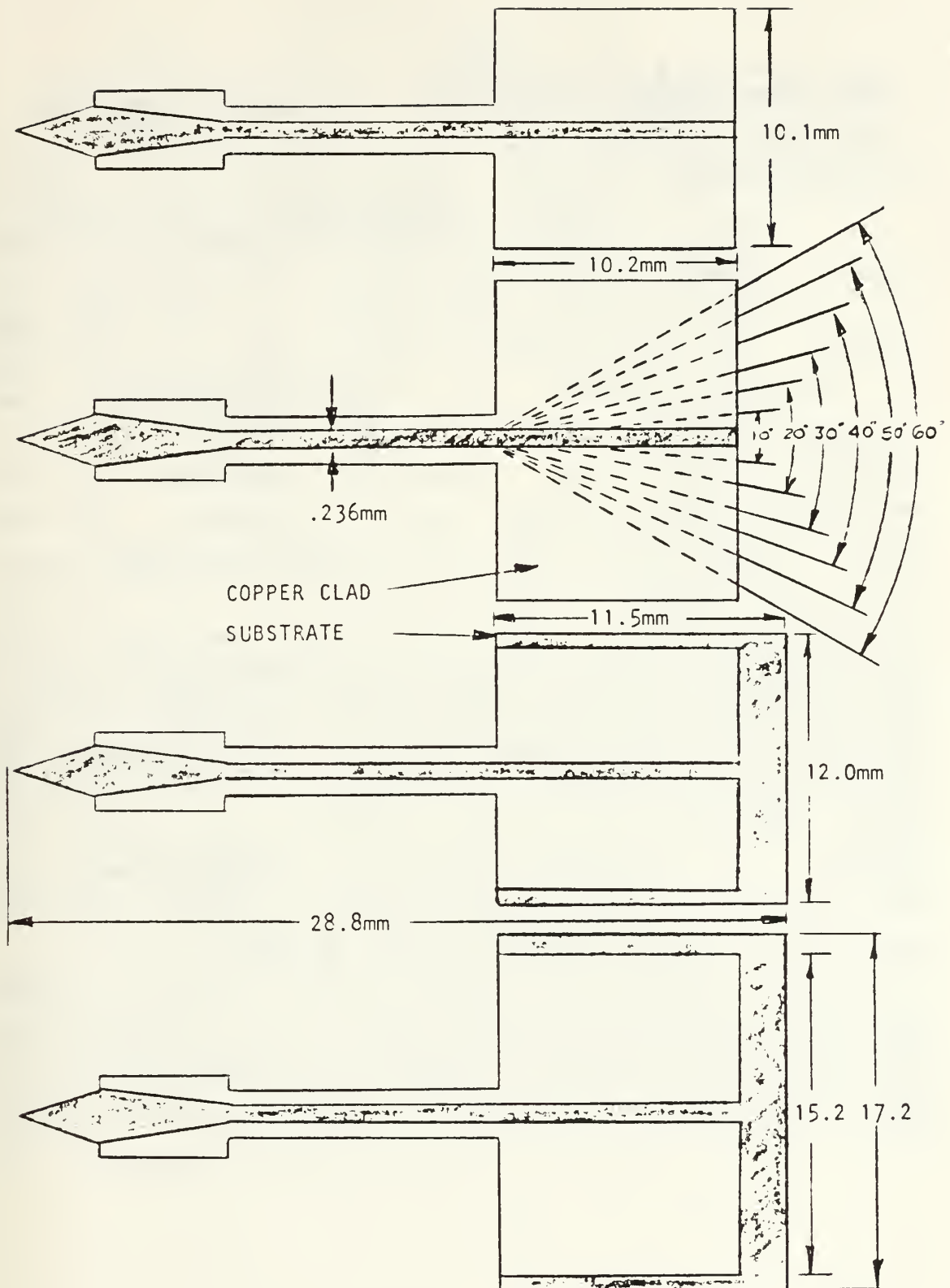


Figure 3.1 Sketch of Test Antennas.

IV. EXPERIMENTAL APPARATUS AND MEASUREMENT PROCEDURES

A. TEST SYSTEM

As stated, a complete data set for each flare angle consists of swept return loss, swept on-axis absolute gain, and E/H-Plane radiation patterns for each of the four antennas, with and without a ground plane. To streamline the measurement process, an integrated test system was assembled and controlled by a desktop computer through a IEEE-488 interface bus. Central to the swept frequency measurements is a scalar network analyzer. Radiation pattern data was taken with a rectangular recorder that was controlled manually. A block diagram of the test set-up is shown in Figure 4.1. Two sweep generators were required in the test set-up because of the different modulation requirements of the HP-8756A scalar network analyzer and the Scientific-Atlanta pattern recorder. The HP-8620C sweep oscillator has an external switch that selects the 1 KHZ square wave required by the pattern recorder where the HP-8350B sweep oscillator requires an internal jumper to make this selection. The HP-8756A requires a 27.5 KHZ square wave that was provided by the HP-8350B.

The test fixture is a modified slotted section of WR(90) waveguide. As shown in Figure 4.3 the slotted guide could be disassembled to permit mounting of an antenna under test. The ground plane was affixed to the end of the guide as shown in Figure 4.5.

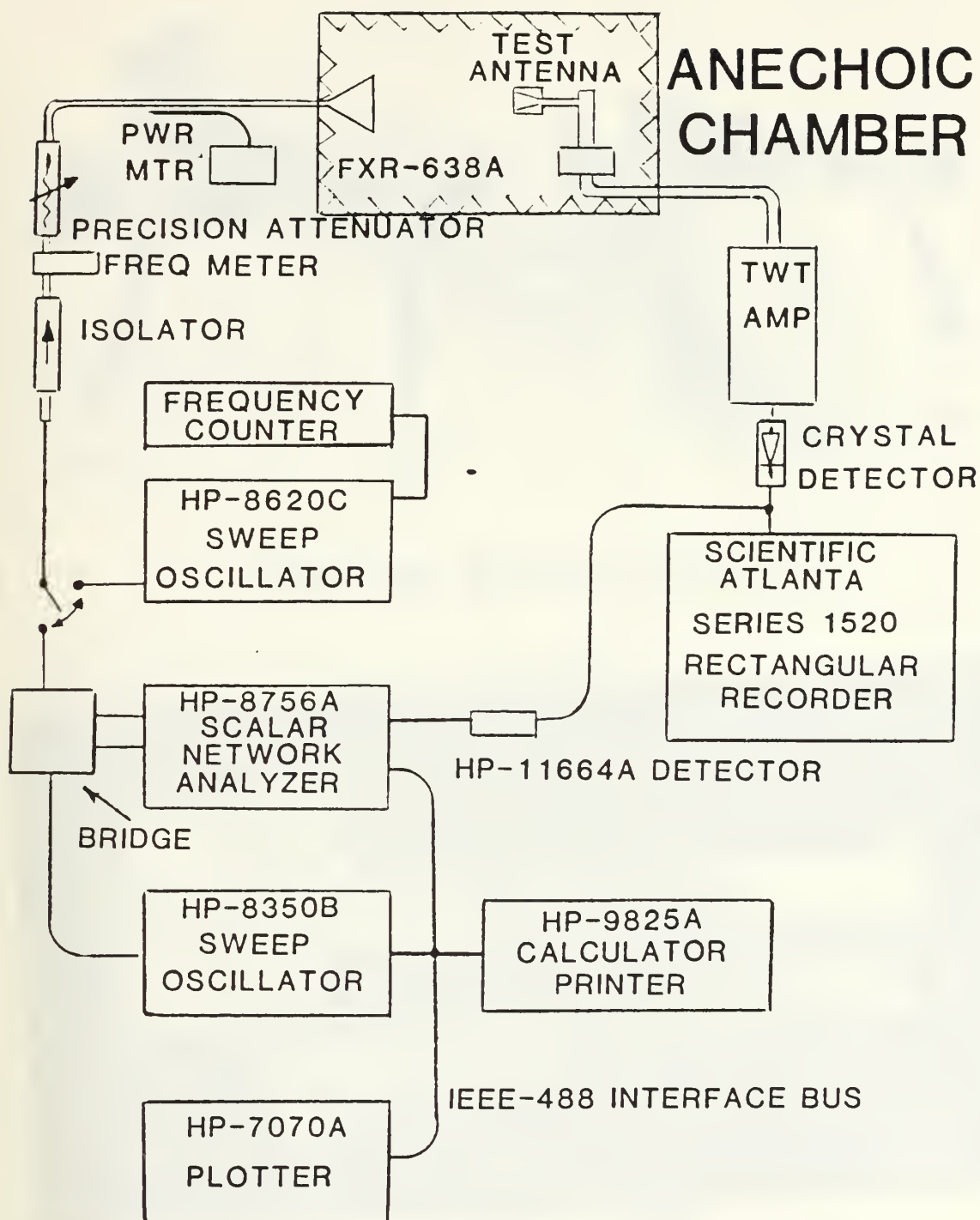


Figure 4.1 Test Set-up.

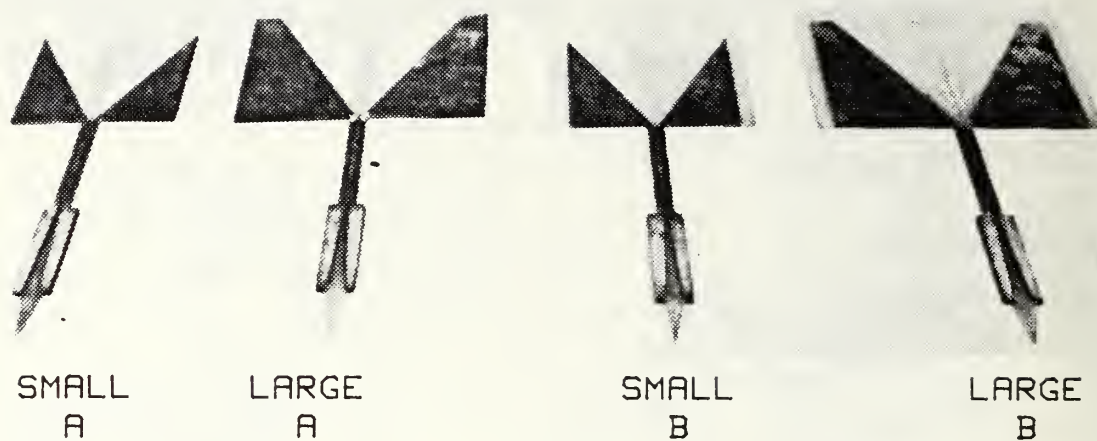


Figure 4.2 Photo of Test Antennas.

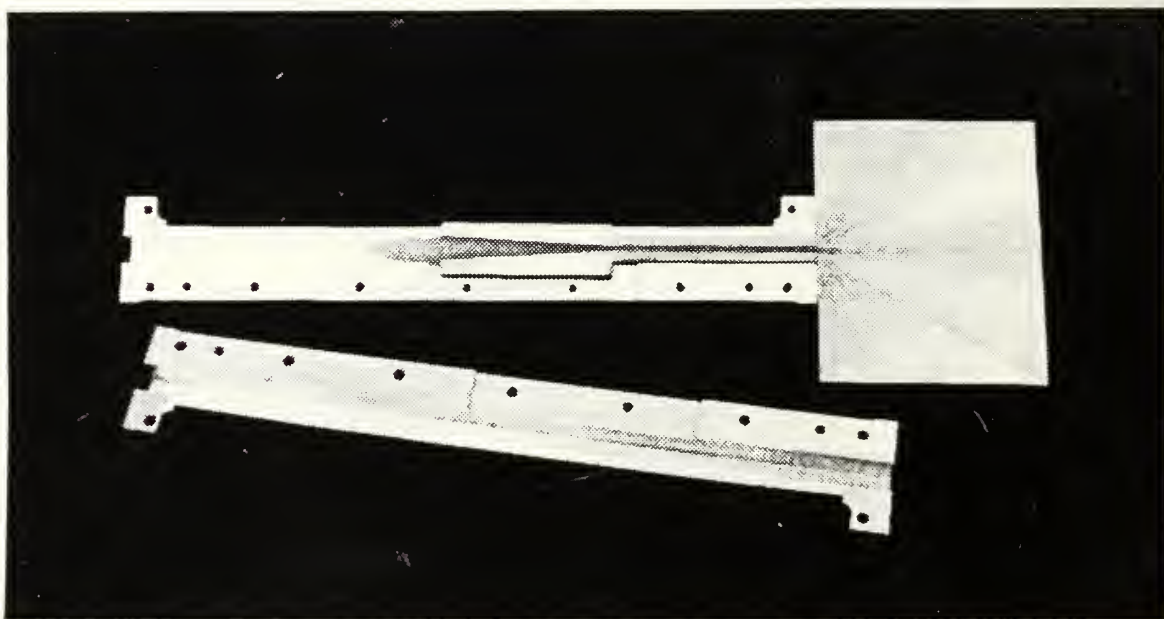


Figure 4.3 Photo of Test Fixture.

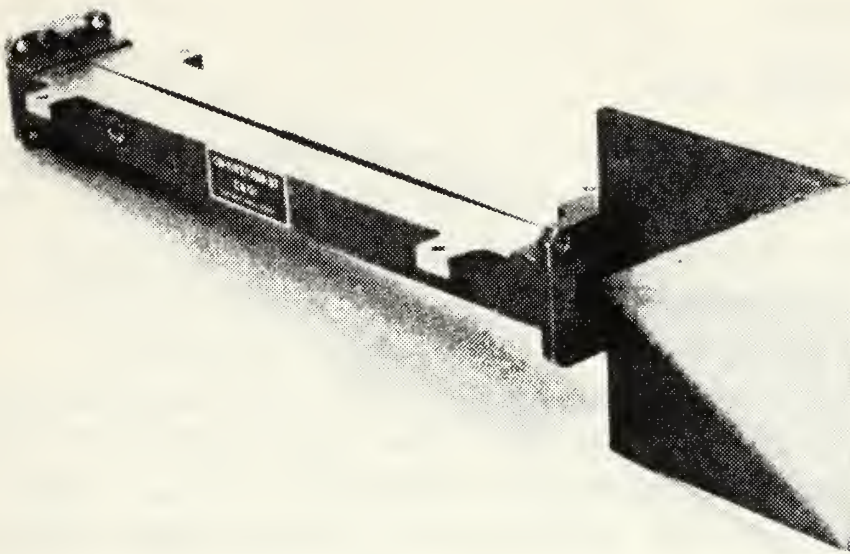


Figure 4.4 Photo of Test Fixture
with With Test Antenna.

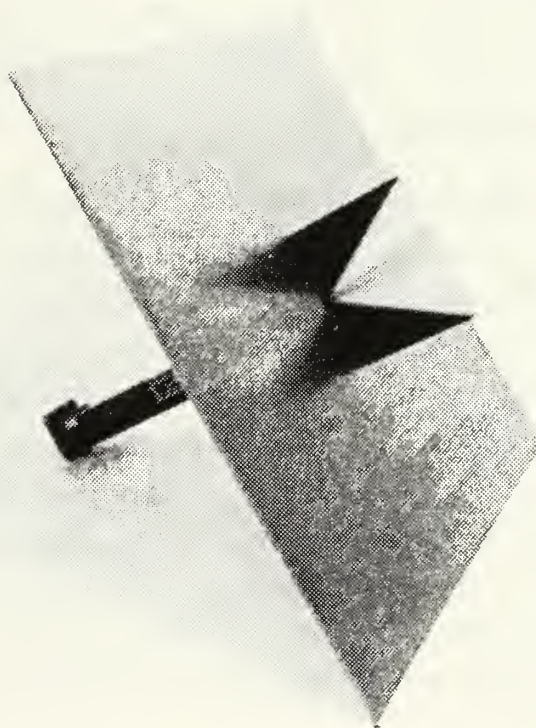


Figure 4.5 Photo of Test Fixture with Ground Plane.

B. PROCEDURES

1. Return Loss

A HP-8756A scalar network analyzer controlled by a HP-9825A calculator collected swept frequency data for return loss and on-axis absolute gain. The computer facilitated plotter operation and performed calculations for absolute gain measurements and subsequent plotting.

For return loss measurements the analyzer was first calibrated using short and open terminations. The test fixture was then connected directly to the reflectometer bridge through the use of a waveguide-to-coax adaptor and the computer program run. This caused the swept frequency data to be displayed and plotted. Figure 4.6 is an example. Shown is the scalar network analyzer plot with the notation A/R for reflection ratio. Figure 4.6 also shows that the typical return loss is greater than 10 dB.

2. Absolute Gain

For absolute gain measurements the analyzer was calibrated by storing the swept frequency transmission ratio data for the Microline 56X1 standard gain horn in the memory of the analyzer. The test antenna, mounted in the fixture as shown in Figure 4.4, was then connected to the receiver antenna mounting in the anechoic chamber. The test antenna trace minus the standard gain antenna trace was displayed and the computer program run. The program controlled the built-in cursor of the analyzer and read 100 points of the resultant trace from 8 to 12 GHz. Each point was entered into the equation for absolute gain where:

$$G = D + 16 + 20\text{Log}_{10}(\text{freq}/9.5) \quad (\text{eqn } 4.1)$$

and

D = Transmission ratio of test antenna (eqn 4.2)

- Transmission ratio of standard gain antenna

The resulting value was printed on an output tape along with the corresponding frequency and then plotted on the HP-7070A plotter. Figure 4.7 is an example.

3. Radiation Patterns

E and H-Plane radiation patterns were recorded using a rectangular recorder at the frequency of maximum gain as determined by the 100 point print out. The standard gain horn pattern was recorded along with the test antenna pattern for comparison. See Figures 5.11 - 5.14.

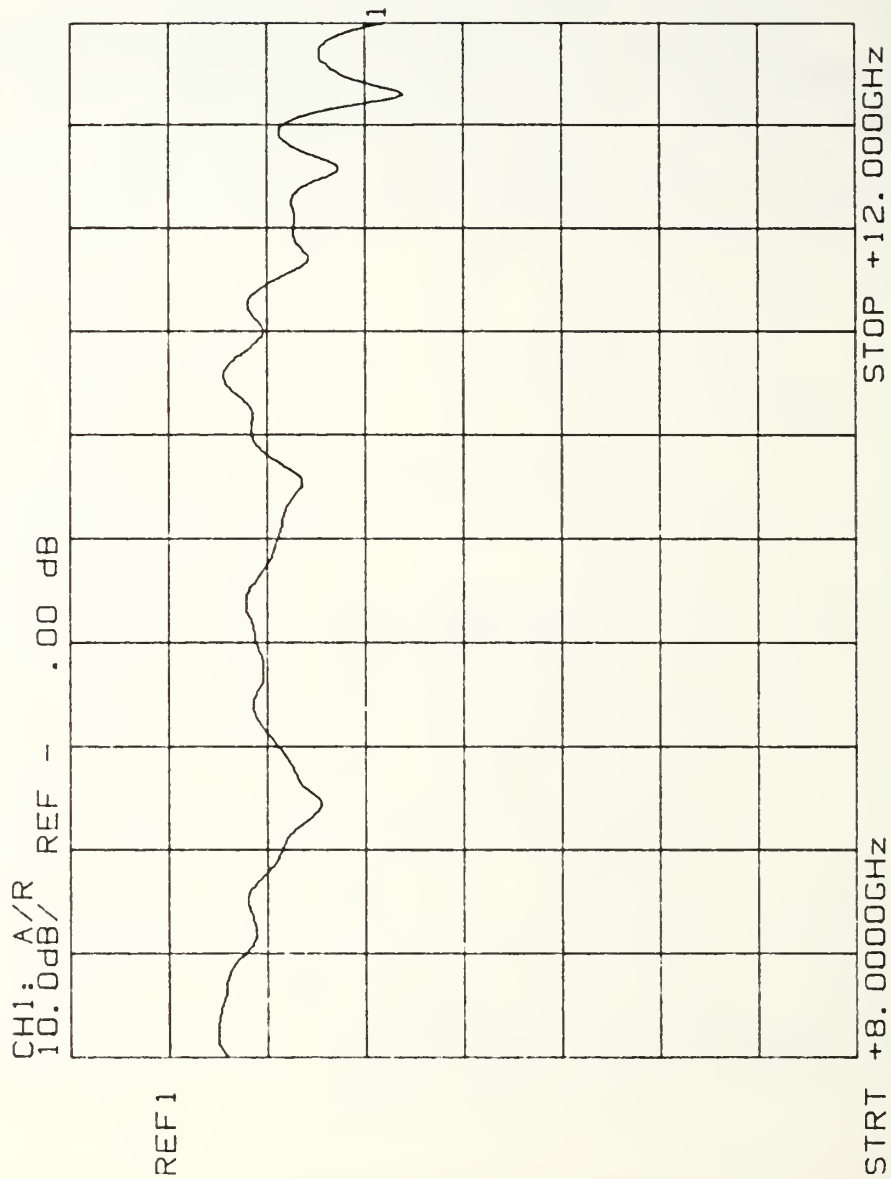


Figure 4.6 Typical Return Loss Plot: 40° Flare Angle and Small B Antenna.

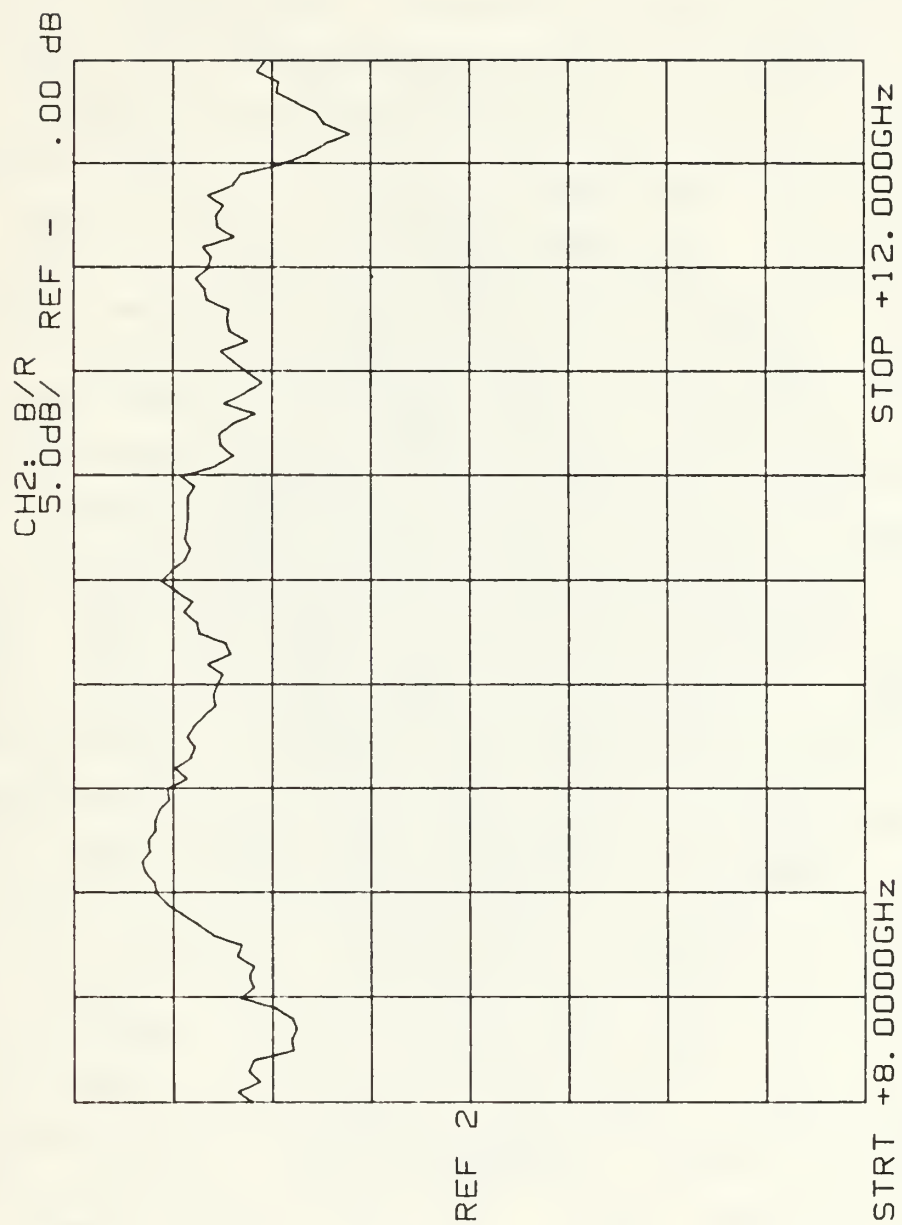


Figure 4.7 Typical Absolute Gain Plot: 400 Flare Angle and Small B Antenna.

V. ANALYSIS

The data collection system produced a substantial amount of measured points for analysis. Summarizing, each of the four antennas had swept frequency return loss and absolute gain data taken for seven different flare angles, with and without a ground plane. In addition, E and H-Plane radiation patterns were taken for all of these cases. Empty waveguide and unextended fin-line reference data added to the quantity. The result was 56 return loss plots, 112 radiation patterns and 6000 absolute gain points.

Return loss data were reduced by hand to determine the effects of mismatch on the measured gain values. A table was made that listed the worse, typical and best values for all four antennas, with and without a ground plane.

To facilitate on-axis gain analysis, it was decided to present the data in graphical form using two different formats. The hope was to present the data in a way that would aid in making comparisons between antenna configurations and designs. One format is three dimensional and displays gain versus frequency versus flare angle for each antenna, with and without a ground plane. See Figures 5.1 through 5.8. Open waveguide data is included on the plots for comparison. It is labeled "wg" on the graphs. A gain profile on the plot shows the graph of the maximum gain values of open waveguide and of each flare angle over the frequency range. The second format is two dimensional and displays gain versus frequency for each antenna, with and without a ground plane, for a particular flare angle. Figure 5.9 is an example that shows the data for all antennas with a ground plane at 40° flare angle. Again open waveguide data is included for comparison.

Gain vs Freq vs Flare Angle

Small A Antenna

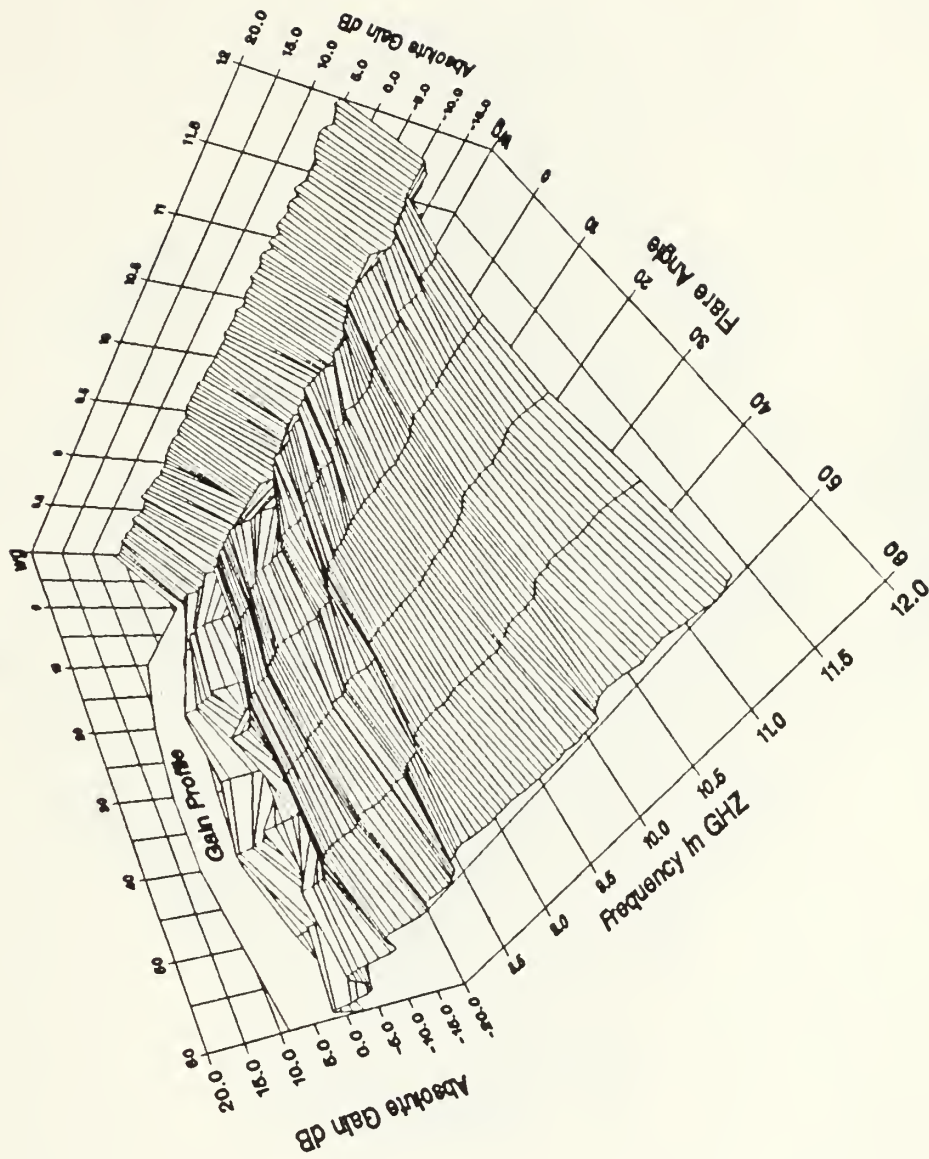


Figure 5.1 Gain Analysis Plot for Small A Antenna.

Gain vs Freq vs Flare Angle

Large A Antenna

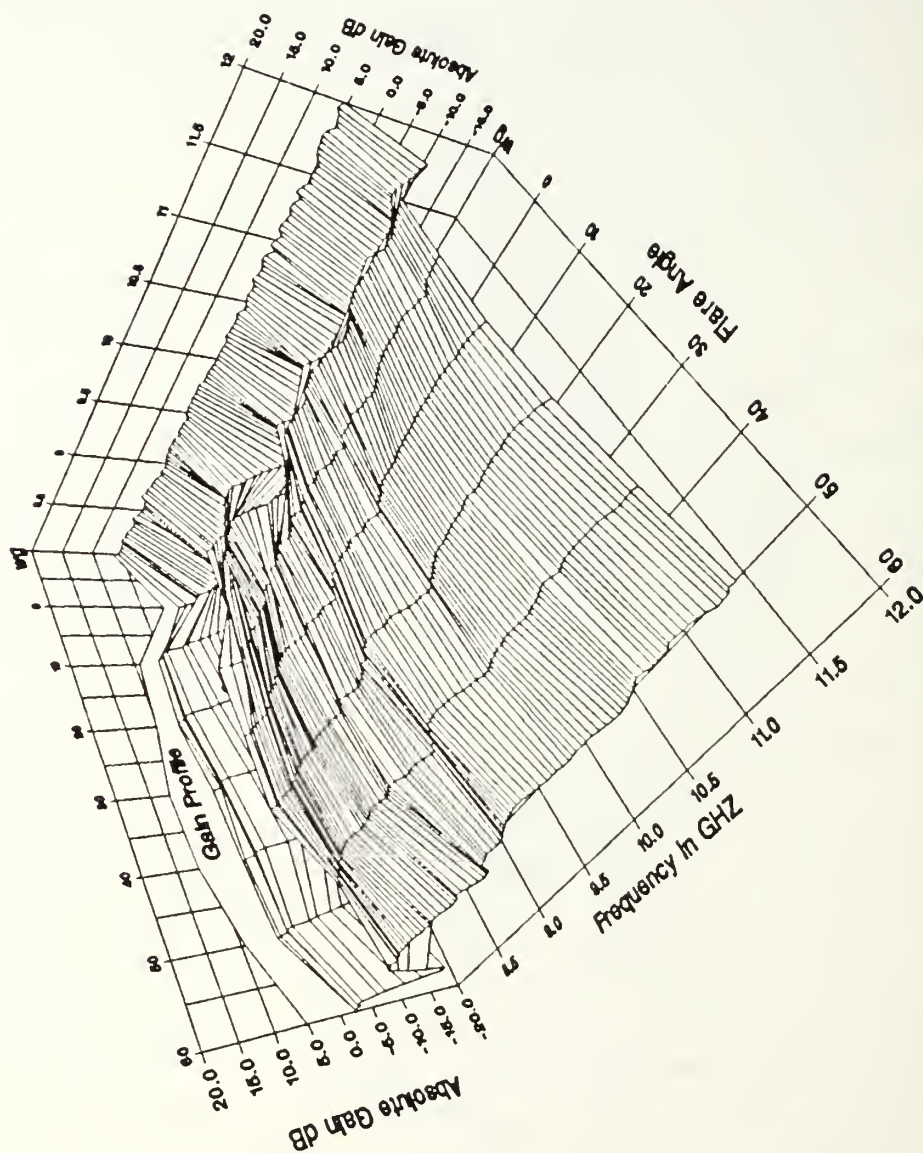


Figure 5.2 Gain Analysis Plot for Large A Antenna.

Gain vs Freq vs Flare Angle

Small B Antenna

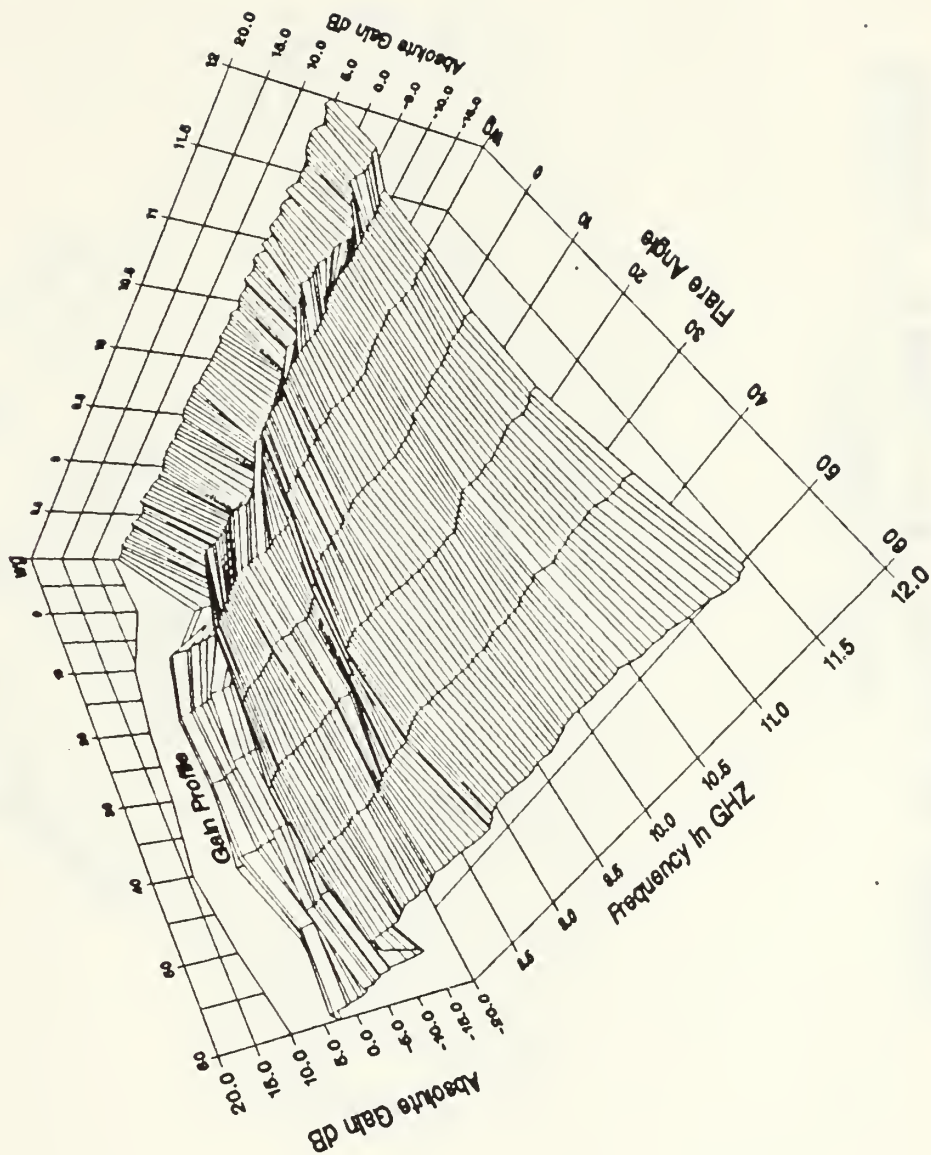


Figure 5.3 Gain Analysis Plot for Small B Antenna.

Gain vs Freq vs Flare Angle

Large B Antenna

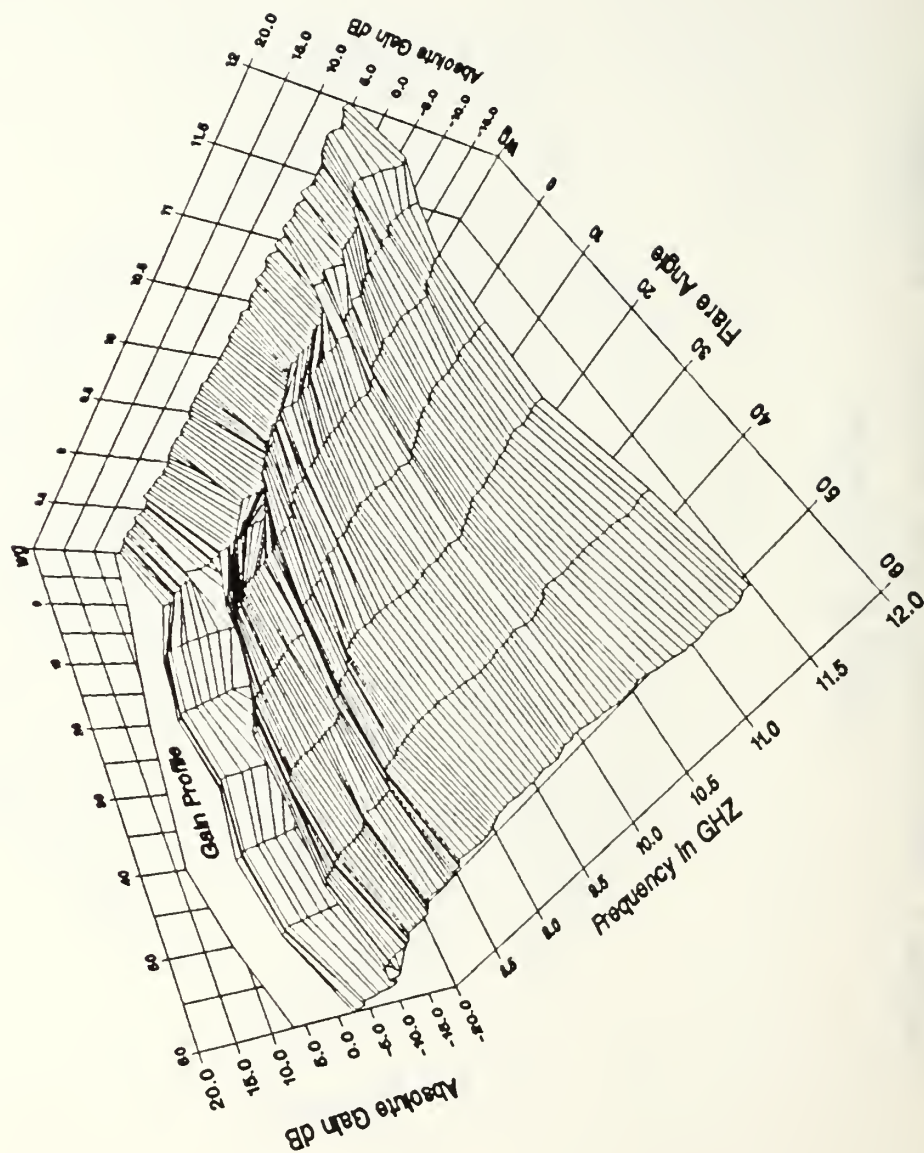


Figure 5.4 Gain Analysis Plot for Large B Antenna.

Gain vs Freq vs Flare Angle

Small A Antenna + G.P.

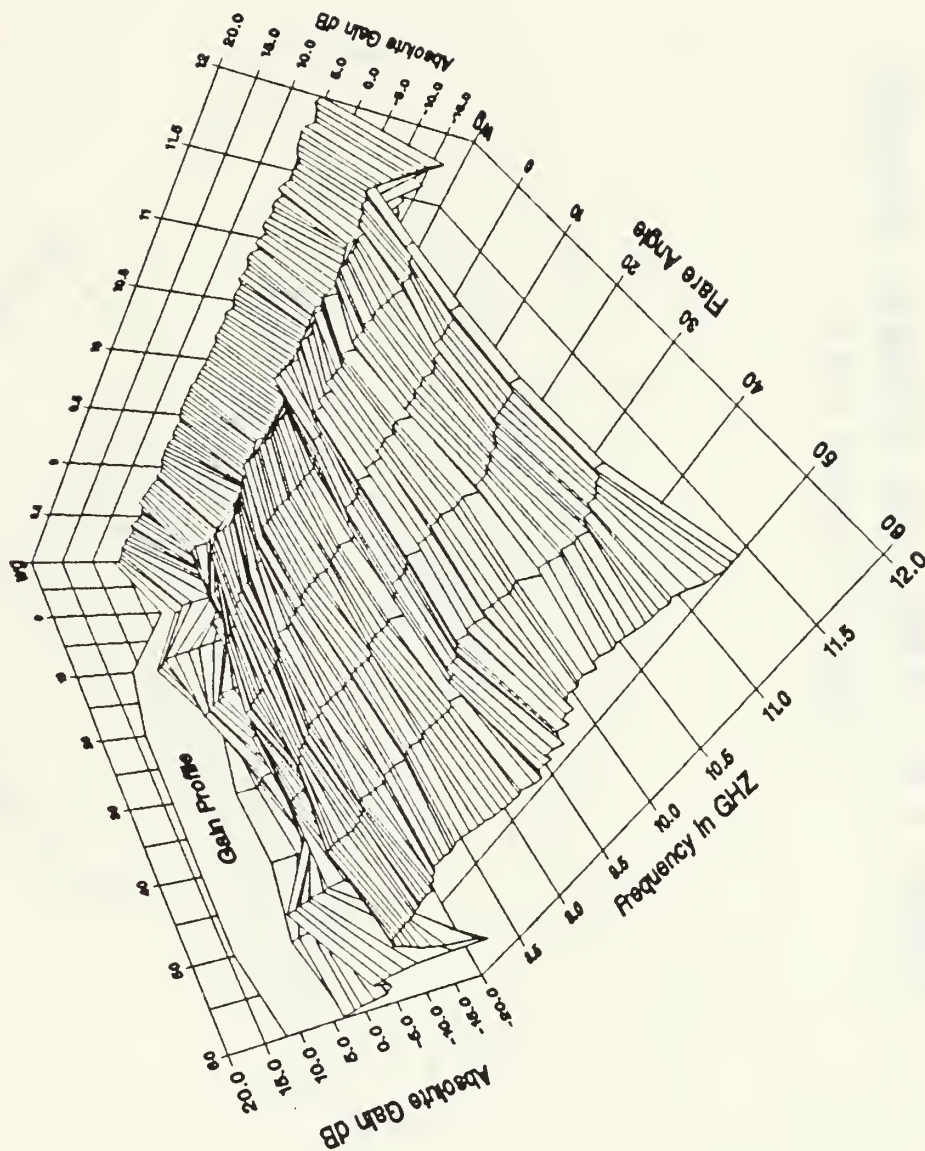


Figure 5.5 Gain Analysis Plot for Small A Antenna Plus Ground Plane.

Gain vs Freq vs Flare Angle

Large A Antenna + G.P.

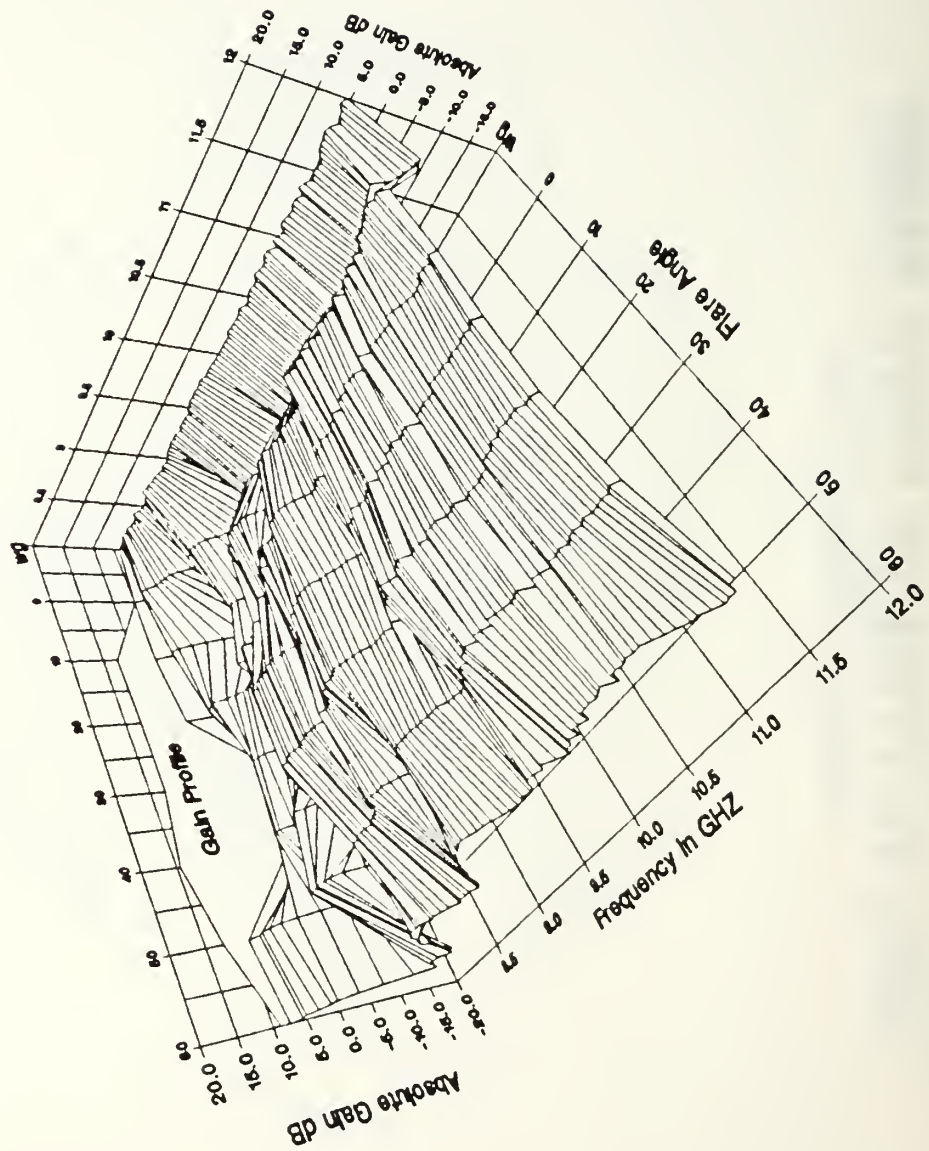


Figure 5.6 Gain Analysis Plot for Large A Antenna Plus Ground Plane.

Gain vs Freq vs Flare Angle

Small B Antenna + G.P.

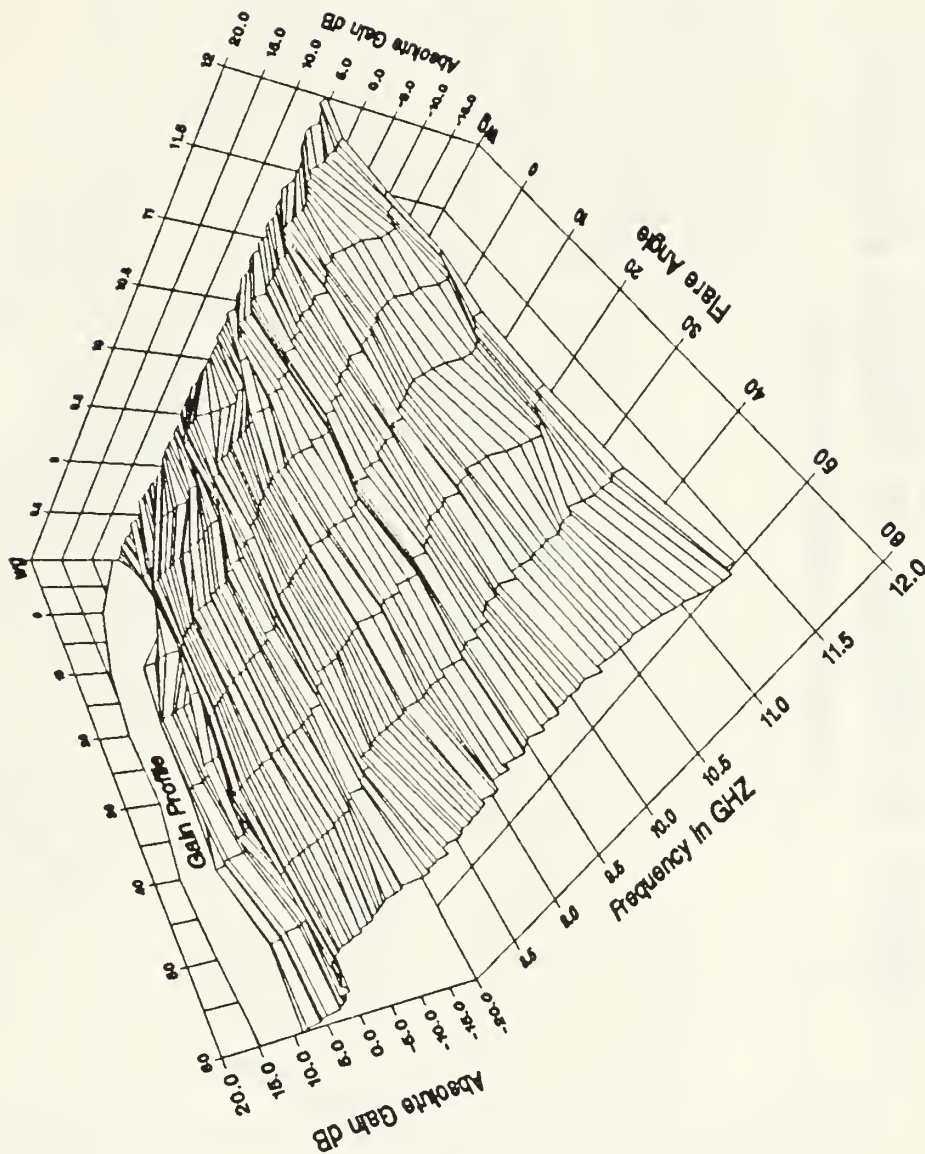


Figure 5.7 Gain Analysis Plot for Small B Antenna Plus Ground Plane.

Gain vs Freq vs Flare Angle

Large B Antenna + G.P.

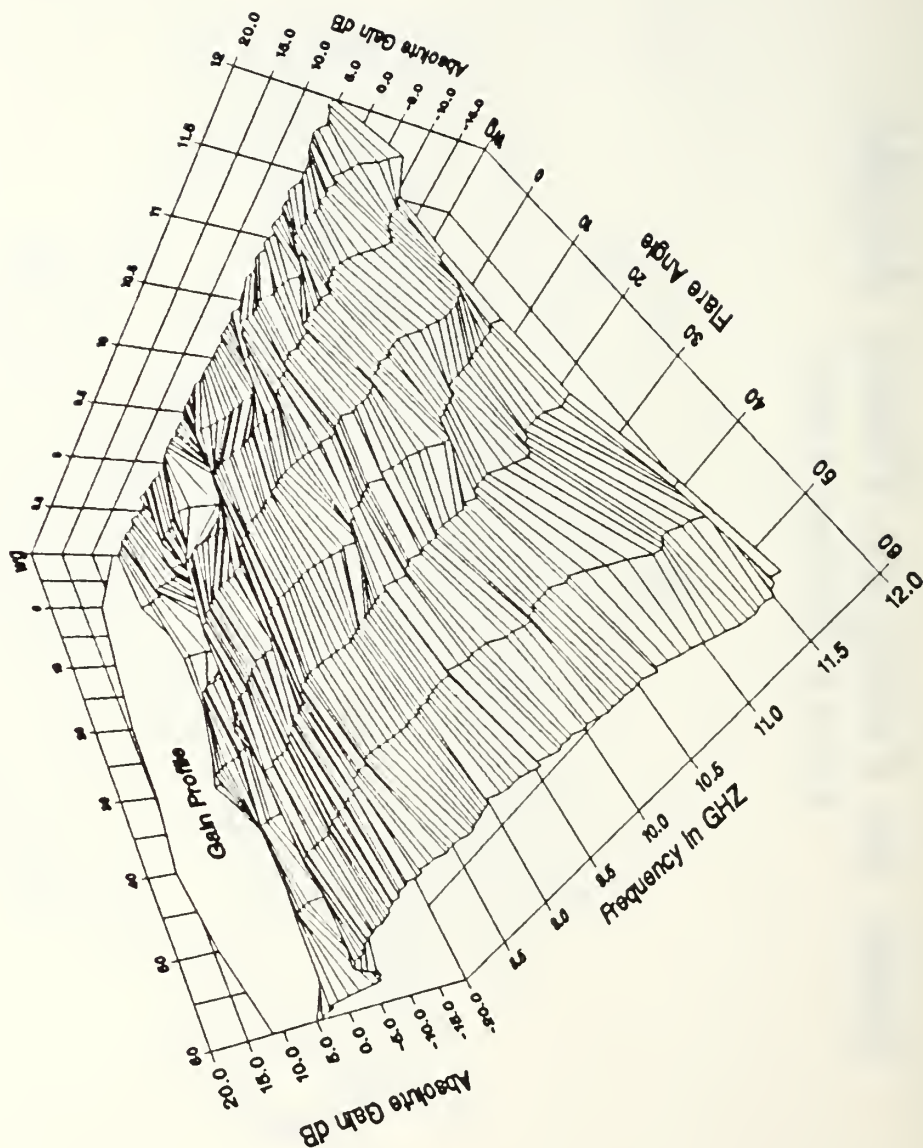


Figure 5.8 Gain Analysis Plot for Large B Antenna Plus Ground Plane.

GAIN VS FREQ FOR ALL ANTENNAS

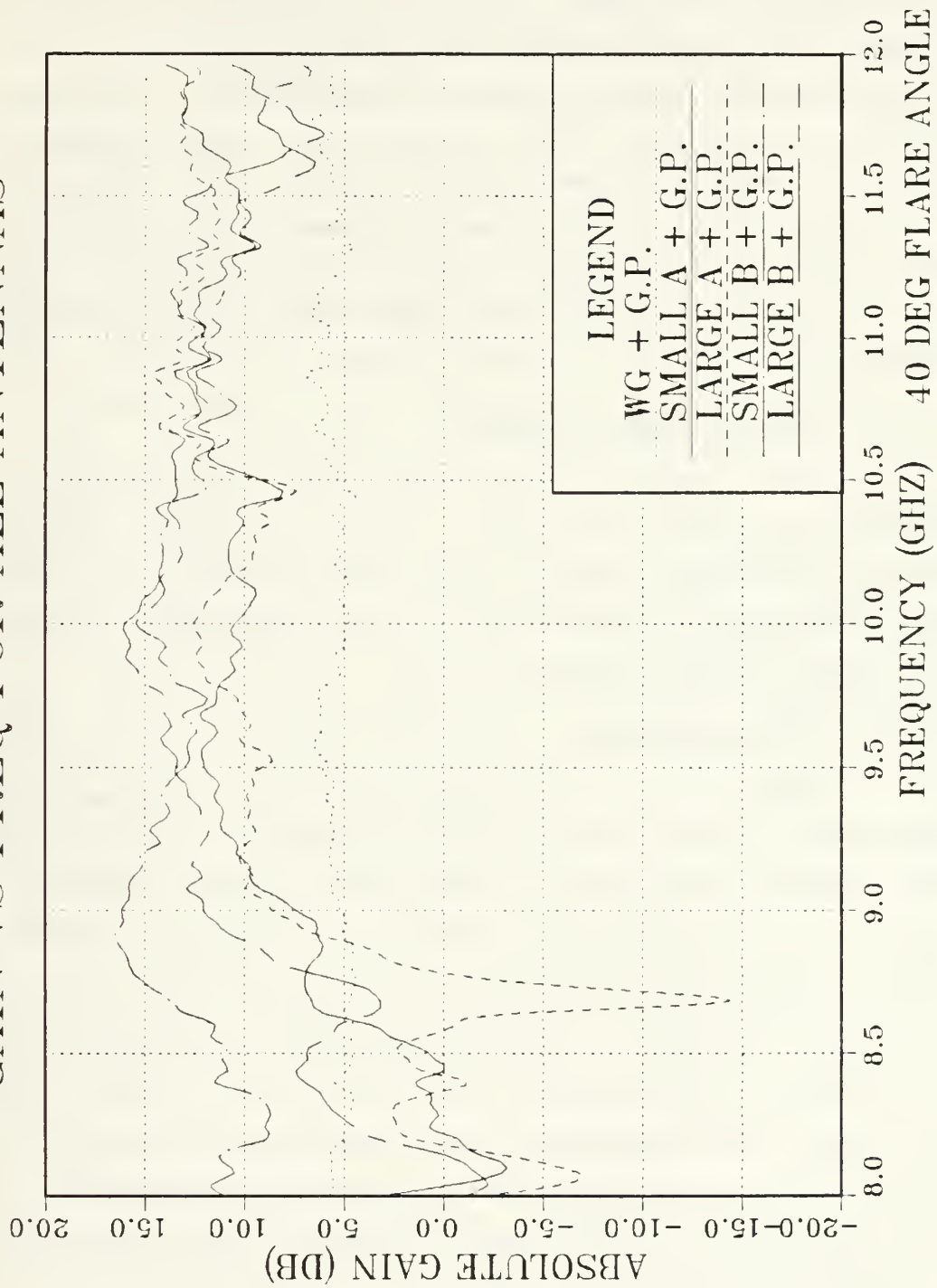


Figure 5.9 Gain Analysis Plot for 40 Degree Flare Angle.

Since no easy method could be determined to enter the gain data into the mainframe computer data files, the 6000 plus numbers were laboriously entered by hand. Once in the data files, computer graphics programs were written to display the data in the formats described.

Radiation patterns were reviewed by overlaying the patterns for a particular antenna, with and without a ground plane, over a light table. The thin plotting paper permitted all seven flare angle plots to be compared to each other. The rectangular format and the standard gain horn trace aided in determining beam width, sidelobe level and on-axis gain.

1. Return Loss Analysis

From the tabular return loss data extracted from curves such as Figure 4.6, it was found that the typical values for return loss in all cases was greater than 10 dB. This translates to less than -.5 dB correction to the absolute gain values measured.

2. Gain Analysis

In Figures 5.1 through 5.8, gain versus frequency versus flare angle is shown for Small A, Large A, Small B and Large B antennas, with and without a ground plane (G.P.). By inspection a number of things are evident with regard to the on-axis gain.

- Absolute gain varies with frequency for a particular flare angle. The roughness of the "gain surface" clearly shows this.
- Data for frequencies less than 9.5 GHz seems to vary widely with deep nulls for gain in this range.
- Zero degree flare angle in general has lower gain than open waveguide.

- Peak gain values increase with increasing flare angle and then fall off with maximum gain occurring between 40° and 50° .
- Increased antenna surface area does not translate into increased gain. In fact, the Large A and Large B antennas showed less gain than their smaller counterparts.
- Addition of a ground plane generally increased gain values for a particular antenna.
- Dielectrically terminated antennas had higher gain than those that ended abruptly with metal.
- Best case antenna overall seems to occur for the Small B antenna plus a ground plane at a 40° flare angle.

It was initially postulated that fin-line horns behave as aperture antennas but a question arose as to appropriate modeling. To a reasonable accuracy standard (0.2 dB), E.H. Braun described a method from which the gain of all electromagnetic horns could be calculated [Ref. 3,4]. Braun's method assumes Huygen source distribution and a uniform, parabolic approximation to describe the equiphase surface at the aperture. As long as the aperture dimensions are on the order of several wavelengths, the gain can be calculated from the physical dimensions of the horn using the universal directivity curves given by Schelkunoff [Ref. 5].

In an attempt to apply the design procedure for three dimensional horns to two dimensional fin-line horns, it was assumed that the test antennas could be modeled as E-Plane sectoral horns with the dimensions as indicated in Figure 5.10. These dimensions, in wavelengths, are those required to compute the predicted gain using Braun's method. The choice of model was based partly on the experimental gain versus frequency versus flare angle data and partly on an intuitive approach. From the theory of gain of horn

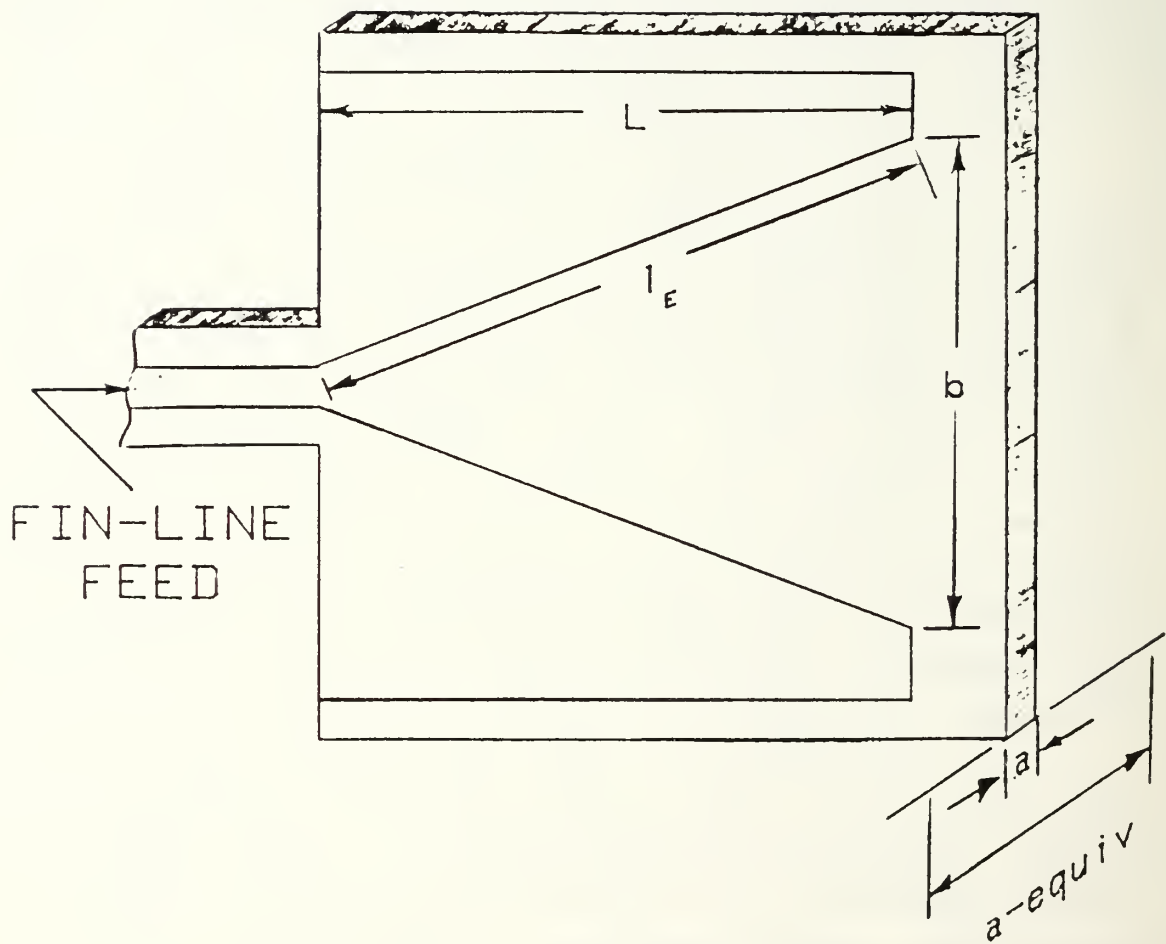


Figure 5.10 Sketch Showing Fin-line Horn Dimensions.

antennas, an optimum flare angle can be derived from the Cornu spiral plot of the Fresnel integral [Ref. 6]. Using horn dimensions, this can be expressed as:

$$\frac{b}{\sqrt{2\lambda L}} \doteq 1.2 \quad (\text{eqn 5.1})$$

For $L = 11.5$ cm and $\lambda = 3.0$ cm, $b = 10.0$ cm this equates to a flare angle of 47° . Gain versus frequency versus flare angle data suggests that a flare angle between 40° and 50° is optimum. This observation suggests that perhaps the fin-line horn behaves as a conventional horn and further motivated the choice of an E-Plane sectoral horn model.

The measured values of gain provided a substantial data base to investigate the possible application of established theory to describe the behavior and predict the gain of fin-line horns.

a. Equivalent a Dimension

As described earlier, the test antennas were constructed from double clad, .125 inch Rexolite 1422. If the actual .125 inch "a" dimension is used to compute the gain for various apertures using Braun's method, the predicted and measured values differ considerably. This observation seemed to indicate that either the assured model is not correct or that there exists some "equivalent a" (a-equiv) dimension. Lacking a basis for a different model, the author opted to search for an a-equiv by working with the experimental gain values. Since the "a" dimension is a constant in three dimensioned sectoral horns, a-equiv was postulated as a value that might also be a constant that would vary as a function of the dielectric constant and thickness of the substrate. Recognizing the the limited accuracy of the measured gain values might affect the a-equiv value, constancy was sought only within the bounds of accuracy of the measurement system.

Computer programs were written to calculate a-equiv by two different methods. The first processed the experimental data for each antenna with and without a ground plane using Braun's method. For example, all of the data for the Small B antenna with a ground plane for frequencies from 8 - 12 GHz and for flare angles from 0° to 60° were applied to the equation:

$$a\text{-equiv} = \frac{g\sqrt{50/l_e}}{G_e} \quad (\text{eqn 5.2})$$

Where

$$g = \text{experimental value of gain} \quad (\text{eqn 5.3})$$

$$G = \text{a value from Schelkunoff curves} \quad (\text{eqn 5.4})$$

The second method used the experimental data to compute effective area from the equation:

$$A\text{-eff} = \frac{g\lambda^2}{4\pi} \quad (\text{eqn 5.5})$$

Dividing A-eff by the corresponding aperture dimension b for each flare angle produced a different a-equiv for consideration. Table 1 shows the values of b and l_e for each flare angle.

In all, each method produced over 5500 a-equiv values that were analyzed for reasonableness and constancy. For a particular antenna, with or without a ground plane, both methods seemed to produce reasonable values but neither seemed to result in values that were consistent for either a particular frequency or a particular aperture. Since return loss data for the antennas was greater than 10 dB in all cases, reflections could not be singled out as the reason for failing to identify a constant a-equiv.

TABLE 1
Antenna Dimensions For Each Flare Angle

<u>Flare Angle</u>	<u>b (mm)</u>	<u>l_e (mm)</u>
0°	2.3	101.6
10°	19.5	106.5
20°	37.5	107.2
30°	56.4	110.0
40°	77.0	112.5
50°	99.0	116.5
60°	102.5	101.5

It appears, then, that the model chosen is not complete and that additional testing is required to determine the phase distribution across the aperture.

3. Radiation Pattern Analysis

As stated, the frequency where maximum on-axis gain occurred determined the frequency where the E and H-Plane radiation patterns were recorded. Since the frequency of maximum gain varied widely (see Figures 5.1 - 5.8), few patterns were taken at the same frequency. This made it difficult to impossible to analyze the effects of flare angle, surface area, end termination and ground plane on the pattern. The 56 E and H-Plane radiation patterns helped correlate the on-axis absolute gain measurements but failure to record patterns at a common frequency was detrimental to the investigation. Still, some general observations were possible. For instance, H-Plane patterns for a particular antenna, with and without a ground plane were remarkably similiar for flare angles from 10° to 60°. That is, 3 dB beamwidths and sidelobes were almost identical. Also, for the best case antenna the following pattern characteristics can be seen in Figures 5.11 - 5.14. Data for Small B with a ground plane are noted in Table 2.

TABLE 2
Small B Antenna Pattern Characteristics

Frequency of pattern	8.92	GHZ
On-axis absolute gain:	Standard gain horn..	15.45	dB
	Test Antenna.....	16.45	dB
H-Plane 3 dB beam width:	Standard gain horn..	32°	
	Test Antenna.....	24°	
E-Plane 3 dB beam width:	Standard gain horn..	28°	
	Test Antenna.....	10°	
H-Plane sidelobe levels:	Standard gain horn..	25	dB down
	Test Antenna.....	10	dB down
E-Plane sidelobe levels:	Standard gain horn..	14	dB down
	Test Antenna.....	9	dB down

CO-POLARIZED

FREQUENCY 10.36GHZ

STANDARD GAIN 16.75 dB

TEST ANTENNA 13.75 dB

3dB BEAMWIDTH 12°

SIDELOBES 5.5 dB DOWN

STANDARD GAIN HORN ANTENNA

FIN-LINE HORN ANTENNA

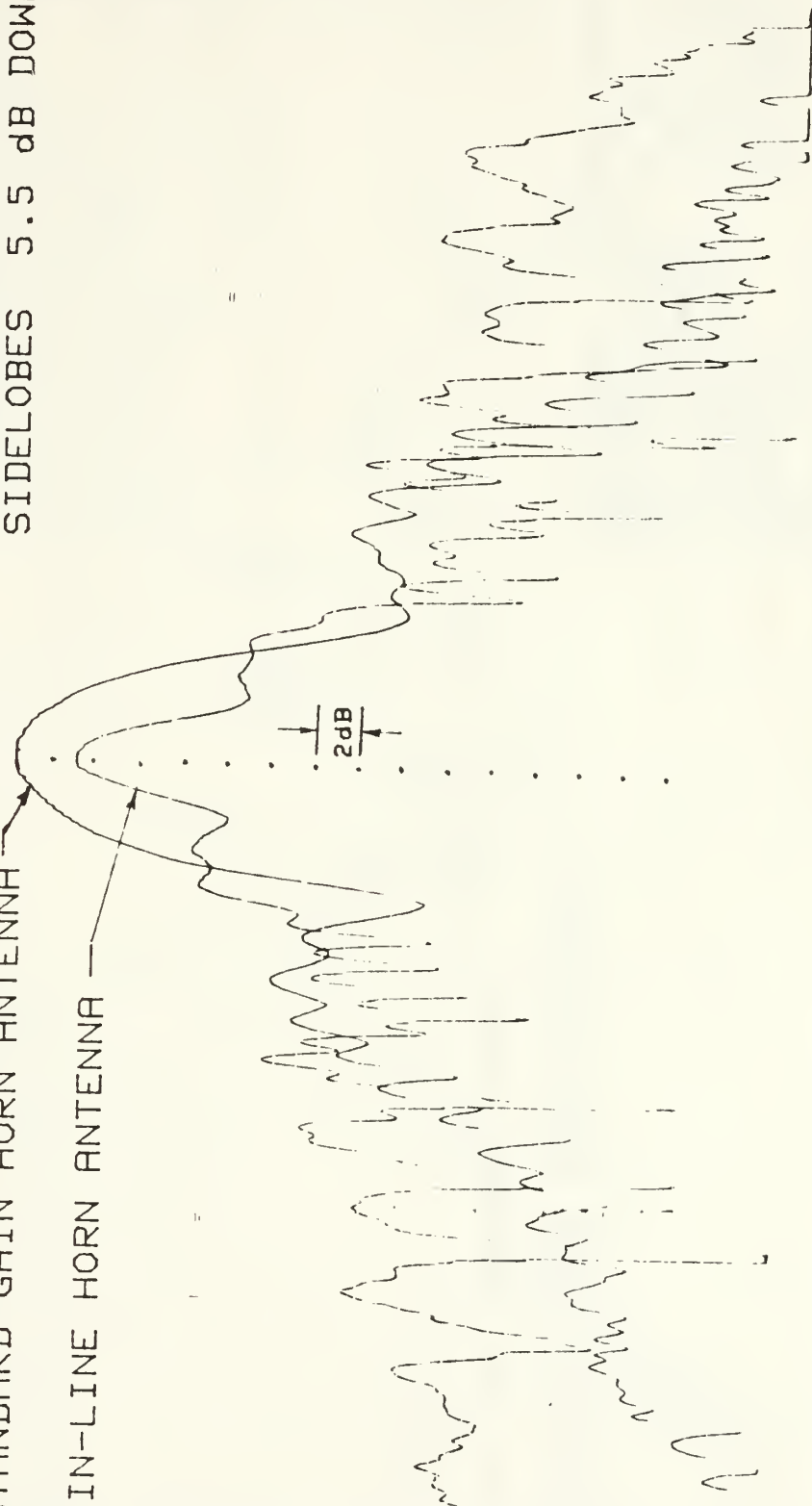


Figure 5.11 E-Plane Radiation Pattern for Small B at 40° Flare Angle.

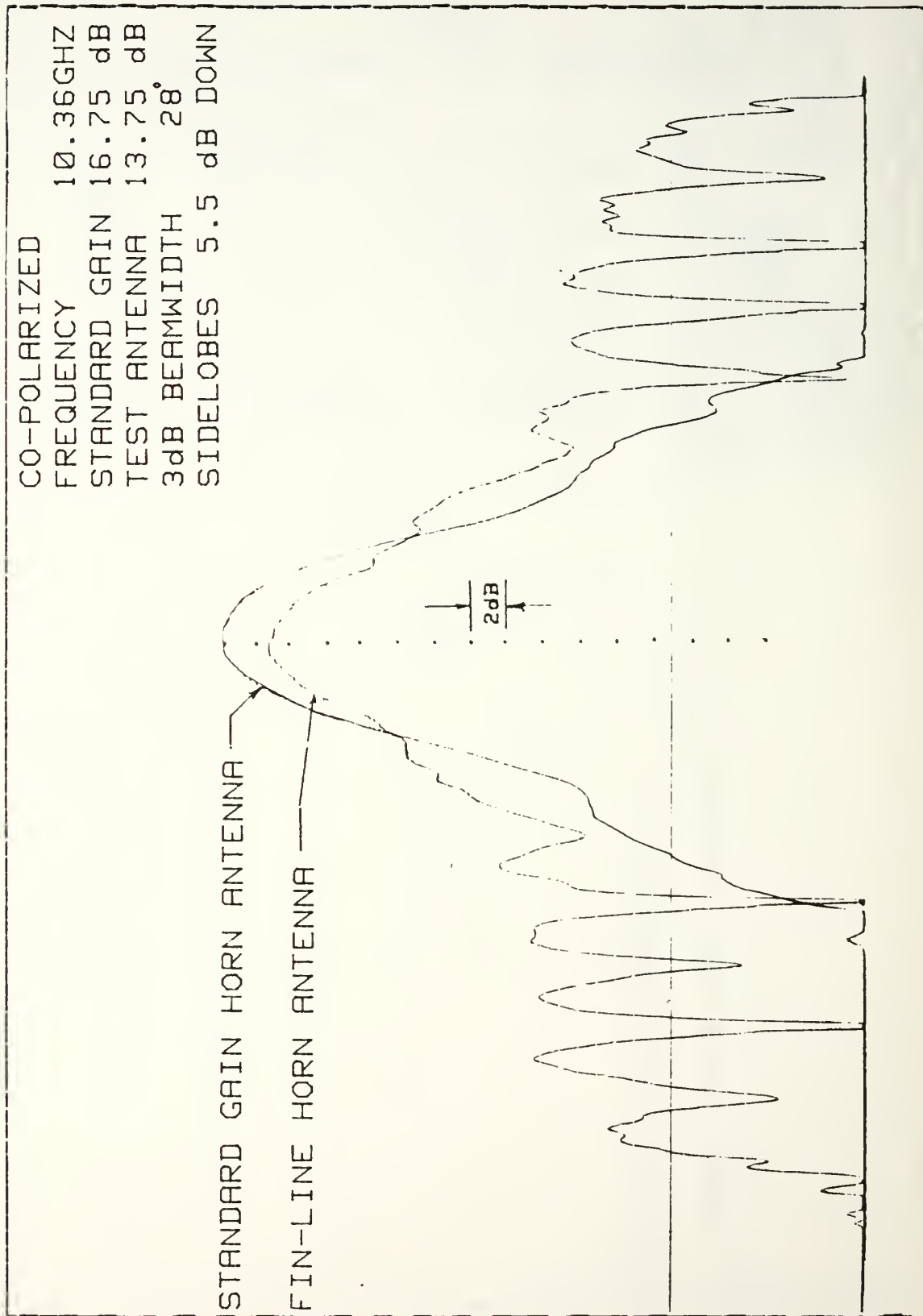


Figure 5.12 H-Plane Radiation Pattern for Small B at 40° Flare Angle.

CO-POLARIZED

FREQUENCY 8.92GHZ

STANDARD GAIN 15.45 dB

TEST ANTENNA 16.45 dB

3dB BEAMWIDTH 10°

SIDELOBES 8.5 dB DOWN

FIN-LINE HORN ANTENNA
STANDARD GAIN HORN ANTENNA

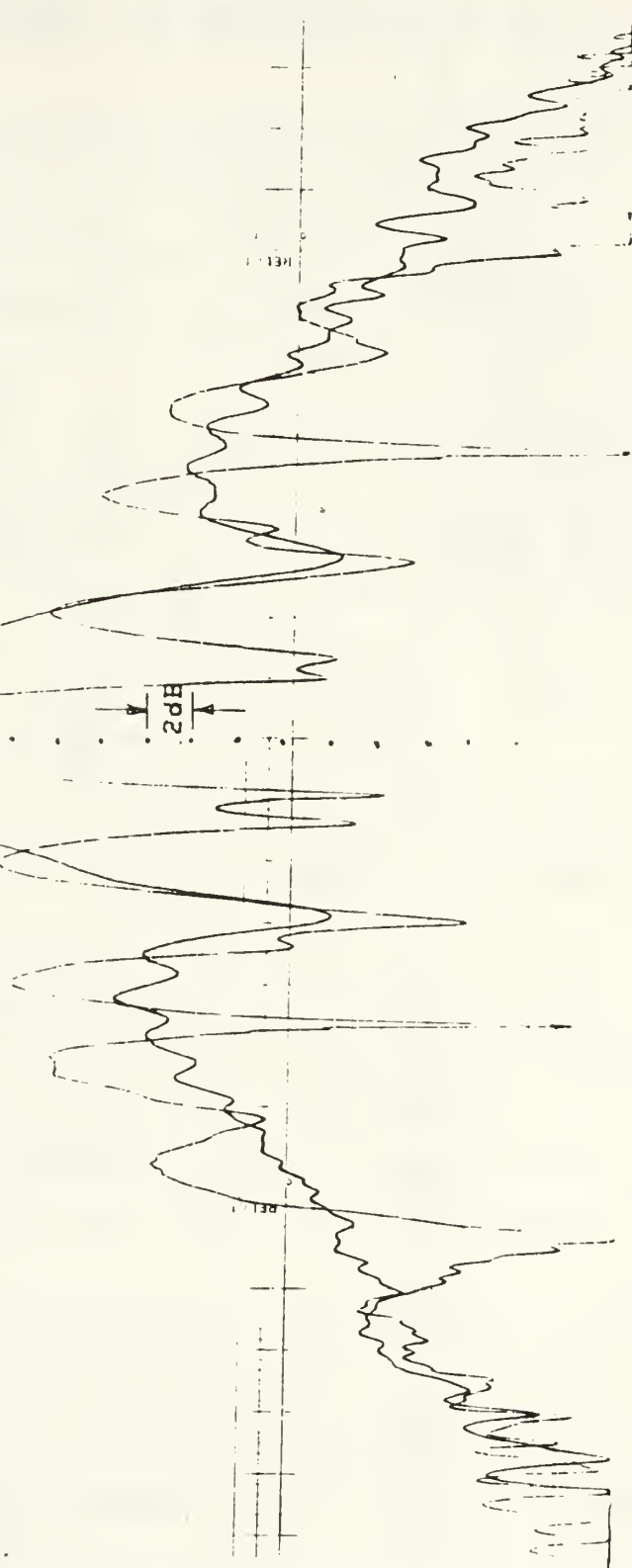


Figure 5.13 E-Plane Radiation Pattern for Small B + G.P. at 400 Flare Angle.

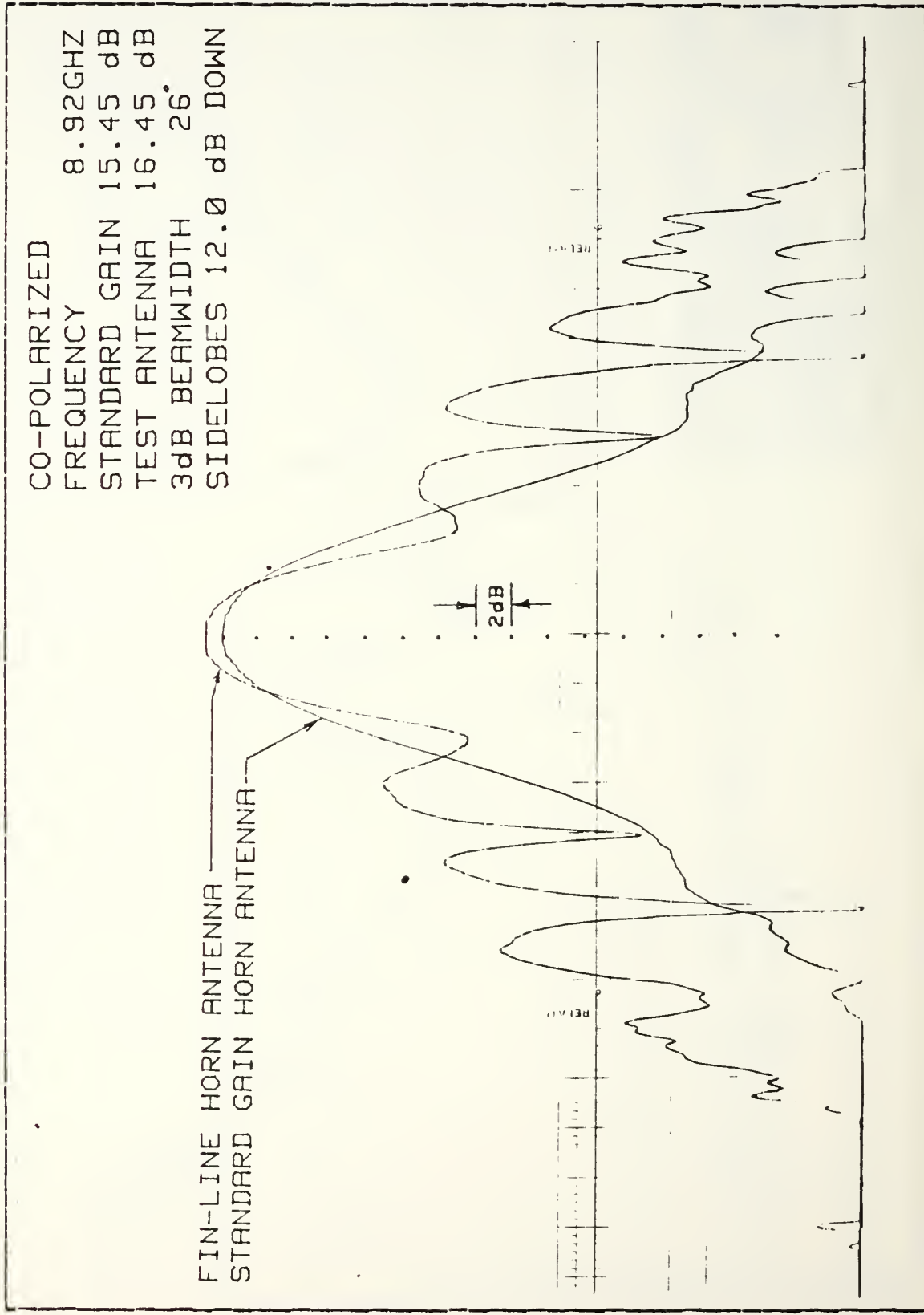


Figure 5.14 H-Plane Radiation Pattern for Small B + G.P. at 400 Flare Angle.

VI. CONCLUSIONS AND RECOMMENDATIONS

The series of experiments conducted on fin-line horn antennas obtained accurate experimental data that will hopefully build on the knowledge of fin-line circuits. This thesis has discussed the analysis of this substantial amount of data and will now summarize the important findings.

With respect to on-axis gain behavior, the following points are concluded:

- Gain varies widely with frequency but generally is highest for mid-range values.
- Gain varies predictably with flare angle with the highest gain for a flare angle between 40° and 50° .
- Increasing antenna surface area decreases gain.
- Dielectrically terminated antennas have higher gain than those that end abruptly with metal.
- The best antenna is one with 200 cm^2 surface area, 40° flare angle, dielectric termination and a ground plane.

With respect to radiation pattern, the following points are concluded:

- H-Plane 3 dB beam widths and sidelobes are insensitive to changes in flare angle for a particular antenna.
- For the 200 cm^2 surface area antenna with dielectric termination and a ground plane (Small B + G.P.), the radiation pattern showed narrow E and H-Plane beam widths, high on-axis gain but undesirably high sidelobes.

This series of investigations verified that fin-line antennas can provide significant gain if configured at a flare angle of 40° and mounted with a ground plane. High sidelobe levels might be troublesome if the antenna is used singly. A better arrangement might be a mechanically

scanned array where the element factor can be suppressed with a resultant overall desirable radiation pattern.

As with all new fields, follow-on experimental studies are needed to refine the theoretical model proposed here. Future studies might examine the aperture phase distribution as well as the effects of flare angle, termination, surface area and dielectric constant on the radiation pattern characteristics.

LIST OF REFERENCES

1. Meier, P.J., "Integrated Fin-line Millimeter Components," IEEE Transactions MTT v. 22, p. 1209-1216, December 1974.
2. Meier, P.J., "Millimeter Integrated Circuits Suspended in the E-Plane of Rectangular Waveguide," IEEE Transactions MTT v. 26, p. 726-732, October 1978.
3. Jakes, W.C., "Gain of Electromagnetic Horns," Proc. IRE v. 39, p. 160-162, February 1951.
4. Braun, E.H., "Some Data for the Design of Electromagnetic Horns," IEEE Transactions Antennas Propagation v. AP-4, p. 29-37, January 1956.
5. Schelkunoff, S.A., Electromagnetic Waves pp. 363-365, D. Van Nostrand, 1943.
6. Weeks, W.L., Antenna Engineering pp. 244-249, McGraw-Hill, 1968.

INITIAL DISTRIBUTION LIST

	No.	Copies
1. Library, Code 0142 Naval Postgraduate School Monterey, California 93943	2	
2. Department Chairman, Code 62 Department of Electrical and Computer Engineering Naval Postgraduate School Monterey, California 93943	1	
3. Professor Jeffrey B. Knorr, Code 62Ko Department of Electrical and Computer Engineering Naval Postgraduate School Monterey, California 93943	2	
4. Professor Michael A. Morgan, Code 62 Mw Department of Electrical and Computer Engineering Naval Postgraduate School Monterey, California 93943	1	
5. Lieutenant Commander John R. Musitano, USNR 14701 Dunbarton Drive Upper Marlboro, Maryland 20870	1	
6. Defense Technical Information Center Cameron Station Alexandria, Virginia 22314	2	

13537 5

21715

Thesis
M98643 Musitano
c.1 Fin-line horn anten-
nas.

21715

Thesis
M98643 Musitano
c.1 Fin-line horn anten-
nas.

thesM98643

Fin-line Horn Antennas.



3 2768 000 99367 9

DUDLEY KNOX LIBRARY